Adsorption 8: 79–87, 2002

Adsorption of Nitrogen on Silica Gel Over a Large Range of Temperatures

LI ZHOU* AND SHUPEI BAI
High Pressure Adsorption Laboratory, Chemical Engineering Research Center
zhouli@public.tpt.tj.cn

YAPING ZHOU AND BIN YANG
Department of Chemistry, Tianjin University, Tianjin 300072, People's Republic of China

Abstract. To study the mechanism of physical adsorption of supercritical gases, the adsorption equilibria of N_2 on silica gel for 103–298 K using 20 K increments and pressures up to 10 MPa were measured. A transition of the adsorption mechanism was proven on crossing the critical temperature, but the transition way observed is different from that observed with activated carbon. This causes a difference in the locations of the linear section of the n-ρ_g isotherm at the near-critical temperature. Although the isotherm type is different on silica gel and on activated carbon in the sub-critical region, all isotherms in the supercritical region can be well modeled by a single model. It leads to the argument that the adsorption mechanism of supercritical gases is identical no matter what kind of adsorbent is used.

Keywords: supercritical adsorption, adsorption mechanism, isotherm modeling, adsorption equilibria, gas/solid adsorption

1. Introduction

Physical adsorption of gases at supercritical temperatures is of growing research interest because of its important industrial application in separation processes (Yang, 1987; Ruthven et al., 1994) or potential industrial application in the adsorptive storage of gaseous fuels (Matranga et al., 1992; Noh et al., 1987; Cannon, 1994). However, the separation coefficient between any two components of a multi-component mixture cannot be thermodynamically calculated, as it can in other separation processes, leads us to the realization that the theoretical fundamentals of these important applications is still very weak. An essential problem in the development of supercritical adsorption theory is to define the state of the adsorbate in the adsorbed phase at above-critical temperatures. Although the liquid state is commonly accepted at sub-critical temperatures, this cannot be true for the supercritical region. Therefore, it is required to investigate the adsorption mechanism under supercritical conditions. Menon summarized the progress in the studies of high-pressure adsorption before 1960's (Menon, 1968). However, considerable progress has been made in measurement techniques during the past 20–30 years (Keller et al., 1995; Lösch, 1999; Humayun and Tomasko, 2000), so that the experimental data reported are more precise and reliable. Most experimental studies on supercritical adsorption are summarized in Table 1. Simulation studies on supercritical adsorption (Vermesse and Levesque, 1994; Matranga et al., 1992; Tan and Gubbins, 1990; Jiang et al., 1994; Chen et al., 1997) have been an important implement to the experimental works. However, the inadequacy of our understanding of intermolecular forces and approximations made for adsorbent geometry remains a significant problem.

Experimental study of supercritical adsorption for a wide range of temperatures covering both the sub- and

---

*To whom correspondence should be addressed.

Table 1. Part of previous experimental studies on supercritical adsorption.

System	Temperature (K)	Pressure (MPa)	Literature
N_2, Ar/Activated carbon	197–293	Up to 40	Menon, 1968
N_2, CO/alumina	197–373	Up to 300	
N_2, Ar/MSC-5A	298–348	Up to 20	Ozawa et al., 1976
CH_4, CO_2/MSC-5A	298–348	Up to 10	
N_2, Ar, CH_4, C_2H_6, C_2H_4, CO, CO_2, N_2O/MS-5A zeolite N_2, Ar/MS-13X zeolite	Most in 273–348; some at 351 or 77	Up to 20	Wakasugi et al., 1981
Ethylene/Graphon	263–323	Up to 12	Findenegg, 1983
Ar, CH_4/Graphon	253–323	Up to 15	Specovius and Findenegg, 1978
Kr /Graphon	253–373	Up to 15	Blümel et al., 1982
CH_4/activated carbon	298	Up to 180	Vidal et al., 1990
Ar, Kr, Ne, N_2, CH_4/activated carbon	298	Up to 650	Malbrunot et al., 1992
Propane/activated carbon	$T < T_c$	6, the highest	Agarwal and Schwarz, 1988
CH_4, N_2/activated carbon	$T > T_c$		
Ethane, ethylene, CO_2/activated carbon	crossing T_c		
H_2/activated carbon	77–298	Up to 6	Zhou and Zhou, 1996
CH_4/activated carbon	298	Up to 5	Chen et al., 1997
CO_2/activated carbon	303–318	Up to 20	Humayun and Tomasko, 2000
CH_4, N_2/activated carbon	158–298 (CH_4) 103–298 (N_2)	Up to 10	Zhou et al., 2001a

the supercritical regions is especially interested. Experiments on activated carbon were first completed (Zhou et al., 2001a). The isotherms in both sub- and supercritical regions show type-I feature and all were satisfactorily modeled by a single model. The adsorption on silica gel presented here shows, however, a different situation. While isotherms in the sub-critical region show type-II feature, the isotherms at high above the critical temperature are quite normal for the supercritical adsorption and, thus a transition in between the two different types of isotherms appeared at near-critical temperature.

2. Experimental

The adsorption equilibrium data were measured on a volumetric set-up shown schematically in Fig. 1. There are two cells, a reference cell and an adsorption cell. The reference cell of known volume was kept in a thermostat, whose temperature was near the room temperature and constant within ±0.1 K. A pressure transmitter model PAA-23/8465.1-200 manufactured by Keller Druckmesstechnik, Switzerland was used to measure its pressure. The deviation from linearity in the whole range of 20 MPa was within 0.05%. The adsorption cell, where adsorbent was loaded, was kept in a cryostat that designed by ourselves, whose temperature was adjustable continuously in the range 77–300 K, and 103.15 to 298.15 K was the temperature range of present study. Details of the cryostat was presented previously (Zhou and Zhou, 1996). The temperature of the cryostat was constant within ±0.1 K at higher temperatures, and ±0.2–0.5 K at lower temperatures. The volume of the void space in the adsorption cell was determined by helium at room temperature. There is a valve between the two cells. The moles of gas

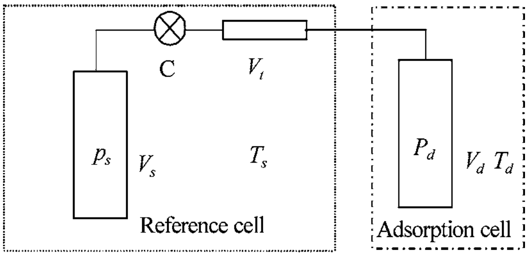

Figure 1. Schematic structure of the experimental set-up.

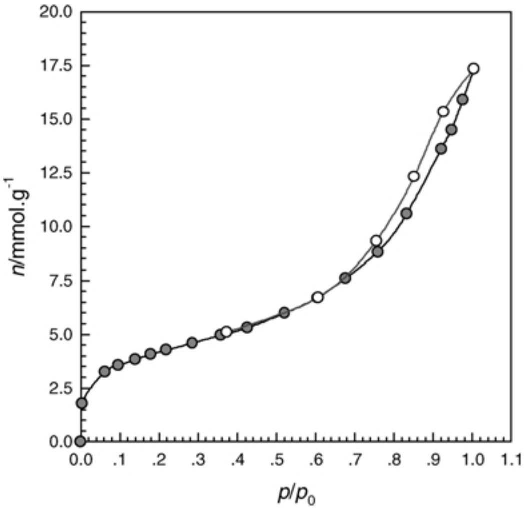

Figure 2. Adsorption isotherm of N_2 on the silica gel sample at 77 K.

confined in each side of the valve were determined by an equation of state of real gases. The amount adsorbed was calculated from the difference of gas moles in the system before and after opening the partition valve. The purity of all experimental gases was higher than 99.99%. A sample of 17.28 g silica gel was used as adsorbent, which is the "silica gel 60" of Merk (Germany) for column chromatography. The adsorption and desorption isotherm of nitrogen at 77 K are shown in Fig. 2. Because the isotherm possessed Type-II feature (IUPAC, 1985) and the hysteresis observed, the silica gel is of meso-porous structure. The specific surface area evaluated by the BET equation (Gregg and Sing, 1982) is 335 m^2/g. The sample had been dried under 10^{-3} Torr vacuum and 393 K for 24 hours before putting in the adsorption cell. The adsorption cell with sample was heated to 393 K and vacuumed again for 6 more hours after having been connected to the apparatus before adsorption measurement.

3. Results and Discussion

The results of the measured excess adsorption are presented respectively in Figs. 3 and 4 and tabulated in Table 2.

3.1. Adsorption Below the Critical Temperature

Two temperatures, 103.15 K and 118.15 K, which are below the critical temperature of nitrogen (126.2 K), were selected for measuring the adsorption equilibrium. The adsorption isotherms obtained are presented in Fig. 3 where the saturated pressure of nitrogen at 103.15 K is 0.953 MPa and 2.27 MPa at 118.15 K (Jacobsen et al., 1986). As in Fig. 2, Type-II feature is clearly shown on the isotherms, so a multi-layer adsorption mechanism is implied.

3.2. Adsorption Isotherms Above the Critical Temperature

3.2.1. Transformation from the Sub- to the Supercritical Isotherms. Nine isotherms were obtained in the range 138.15–298.15 K using 20 K increments as shown in Fig. 4. The isotherms are noticeably different from the sub-critical. Type-I feature is shown on isotherms for higher temperatures. A maximum was shown on isotherms for lower temperatures. "Negative adsorption" was recorded at 138.15 K. Type-II shape can still be noticed for the first section before the isotherm dropped down abruptly if we enlarged the isotherm for 138.15 K separately. Because 138.15 K is the temperature closest to the critical in the experiments, the isotherm behavior observed at 138.15 K may bear a transition feature between the sub-critical adsorption and the supercritical adsorption. The drastic decrease of the isotherm from its maximum was reported previously (Findenegg, 1983; Thommes et al., 1995), and was also observed at the adsorption isotherm of methane on silica gel at 198.15 K (Zhou et al., 2001b). To observe the transition feature more clearly, this isotherm was expressed in Fig. 5 as a plot of n-ρ_g, the excess adsorption vs gas phase density. The isotherm on activated carbon at the same temperature (Zhou et al., 2001c) is also shown for a comparison. A linear section is usually identified for such an expression (Menon, 1968), as clearly shown by the isotherm on activated carbon. The linear section is coincided with the tangent of the isotherm arch on activated carbon because there is not a transformation of isotherms on crossing the critical temperature. However, there is a transformation of isotherm types from type-II in the sub-critical region to type-I in the supercritical region on silica gel leaving a transition section between the two types of isotherms at the near-critical temperature. As consequence, the linear section can no longer be the tangent of the isotherm arch. It is important to identify the difference in the locations of the linear section of isotherms between the two kinds of adsorbents because the linear section defines a limit quantity of

Table 2. The measured adsorption data.

$T = 103.15$ K		$T = 118.15$ K		$T = 138.15$ K		$T = 158.15$ K		$T = 178.15$ K		$T = 198.15$ K		$T = 218.15$ K		$T = 238.15$ K		$T = 258.15$ K		$T = 278.15$ K		$T = 298.15$ K	
P	n	P	n	P	n	P	n	P	n	P	n	P	n	P	n	P	n	P	n	P	n
0.0090	1.7016	0.0350	1.1909	0.0565	0.7289	0.0815	0.5128	0.0995	0.3535	0.1270	0.2454	0.1385	0.1628	0.3351	0.1716	0.2316	0.0881	0.3016	0.0870	0.2921	0.0599
0.0555	2.4884	0.1750	2.1888	0.2251	1.3557	0.2776	1.0171	0.2781	0.6840	0.3211	0.4675	0.3536	0.3094	0.8257	0.3634	0.8197	0.2645	0.8547	0.2162	0.9292	0.1736
0.1385	3.1001	0.4181	2.9098	0.4741	1.9264	0.5732	1.4441	0.4916	0.9631	0.5722	0.6768	0.6222	0.4592	1.4144	0.5461	1.6899	0.4723	1.9775	0.4269	1.7295	0.2961
0.2391	3.8016	0.6622	3.5501	0.8422	2.4146	0.9207	1.7595	0.7417	1.2011	0.8882	0.8897	0.9688	0.6255	2.2086	0.7379	2.6462	0.6434	2.9533	0.5698	2.5457	0.4105
0.3246	4.3635	0.9072	4.1570	1.2763	2.7677	1.4054	2.0471	1.0978	1.4608	1.3088	1.0959	1.4199	0.7996	3.1678	0.9130	3.7200	0.7986	4.0126	0.7075	3.5809	0.5300
0.4036	4.9069	1.1563	4.8797	1.8700	3.1254	2.0595	2.3164	1.5844	1.7228	1.9675	1.3324	2.1091	1.0010	4.2566	1.0575	5.1329	0.9490	5.1569	0.8107	4.6832	0.6440
0.4776	5.6015	1.4279	5.5402	2.5667	3.4415	2.7822	2.5471	2.2446	1.9912	2.7272	1.5518	2.9343	1.1814	5.3174	1.1470	6.4542	1.0432	6.6102	0.9233	5.8846	0.7370
0.5601	7.0321	1.7029	6.6269	3.2519	3.4612	3.5784	2.7308	3.0958	2.2226	3.5824	1.6955	3.8395	1.3127	6.5057	1.2196	7.7080	1.1107	8.2102	1.0096	7.2389	0.8242
		1.8965	8.3255	3.8870	2.5947	4.3987	2.7603	4.0556	2.4155	4.5972	1.8036	4.7903	1.4249	7.7160	1.2609	8.7803	1.1442	9.3780	1.0512	8.6988	0.9059
		1.9605	11.2383	4.5067	0.0237	5.2459	2.5816	5.1654	2.5180	5.7050	1.8807	5.8570	1.4806	8.8238	1.2806	9.5295	1.1653	9.9426	1.0720	9.7416	0.9525
				5.0683	−1.4440	6.1206	2.2328	6.2752	2.5276	6.8003	1.8634	6.9408	1.5138	9.4265	1.2818	9.8961	1.1651			10.2472	0.9717
				5.6540	−1.5107	7.0184	1.7070	7.3729	2.3523	7.9541	1.7735	8.0721	1.5112							10.4908	0.9793
				6.4117	−2.3643	7.6990	1.2406	8.1426	2.1585	8.6738	1.7309	8.8093	1.4895								
				7.3374	−2.7854	8.3707	0.5768	8.8203	1.9830			9.3140	1.4707								
				8.3577	−3.0732	8.9584	0.0057	9.2679	1.8921												
				9.1664	−3.4345																

P in MPa; n in mmol N_2/g silica gel.

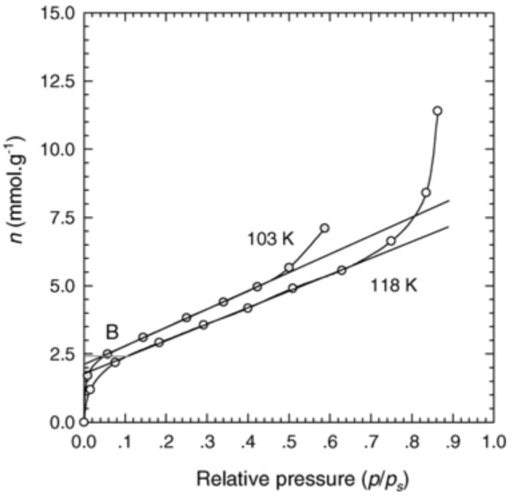

Figure 3. Sub-critical adsorption isotherms of nitrogen on silica gel.

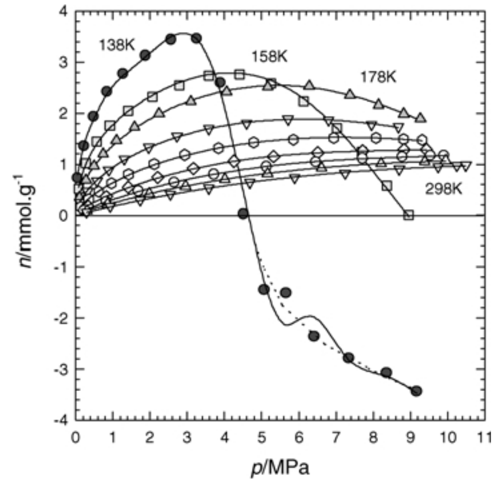

Figure 4. The excess adsorption isotherms of supercritical N_2 on silica gel Dots: experimental; Curves: model-predicted.

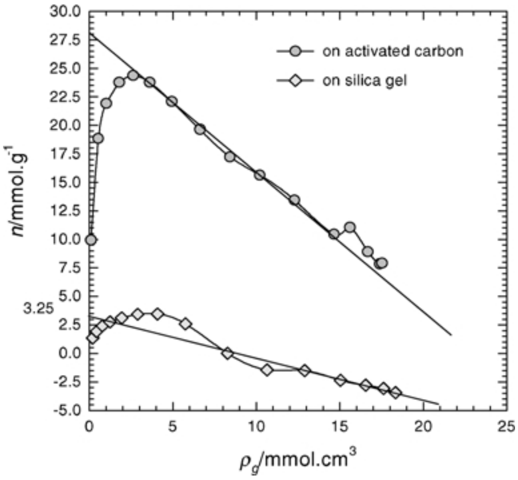

Figure 5. The isotherms near the critical temperature against gas phase density.

supercritical adsorption. The linear section isotherm must follow the Gibbs definition of adsorption:

$$n = V_a(\rho_a - \rho_g) = n_t - V_a \rho_g \tag{1}$$

where n is the measured (excess) adsorption, n_t is the absolute adsorption, V_a and ρ_a are the volume and density respectively of the adsorbed phase, and ρ_g is the gas phase density. The quantity n_t, V_a and, therefore, ρ_a must be constant if the relation between n and ρ_g is linear. A limit state of the supercritical adsorbed phase is, thus indicated. The gas phase density keeps increasing while the density of the adsorbed phase keeps constant with the increasing pressure, so a thermodynamically unstable state appears when the former is greater than the latter. Adsorption mechanism ceased to function when the unstable state collapsed at last. The limit quantity of supercritical adsorption on silica gel is 3.25 mmol/g given in Fig. 5 by the intercept of the extended linear section of the isotherm.

3.2.2. Mathematical Model of the Supercritical Isotherms.

It was shown that all isotherms in both sub- and supercritical regions on activated carbon were satisfactorily modeled by a single model (Zhou et al., 2001c):

$$n = n_t^0[1 - \exp(-bp^q)] - \left(\sum_{i=1} c_i p^i\right) \cdot \left(\sum_{j=0} c_j p^j\right) \tag{2}$$

The first term on the right hand side (rhs) is the absolute adsorption, n_t, expressed in a new isotherm equation proposed by the authors (Zhou et al., 2001d). The second rhs term is the product of the gas phase density, $(\sum_{i=1} c_i p^i)$, and the volume of the adsorbed phase, $(\sum_{j=0} c_j p^j)$. The former was determined by an equation of state and correlated with pressure by a polynomial function for each temperature, whose correlation coefficients are given in Table 3; the latter was calculated from the relation shown in Eq. (1):

$$V_a = \frac{n_t - n}{\rho_g} \tag{3}$$

Table 3. Coefficients in the gaseous nitrogen density correlation.

T (K)	c_i						
	c_1	c_2	c_3	c_4	c_5	c_6	c_7
138.15	−0.047226	2.45193	−1.9619	0.70477	−0.11827	0.0093061	−0.00027926
158.15	0.76669	0.033258	6.9212×10^{-4}	1.4812×10^{-3}	-1.3707×10^{-4}		
178.15	0.68085	0.015660	2.9603×10^{-3}	-2.1627×10^{-4}			
198.15	0.60725	0.012870	4.8976×10^{-4}	-5.7697×10^{-5}			
218.15	0.55104	8.3298×10^{-3}	7.8727×10^{-6}	-2.1139×10^{-5}			
238.15	0.50475	5.1133×10^{-3}	-9.3498×10^{-5}	-9.2637×10^{-6}			
258.15	0.46561	3.0846×10^{-3}	-1.2793×10^{-4}	-2.7487×10^{-6}			
278.15	0.43213	1.6971×10^{-3}	-1.1194×10^{-4}	-8.5544×10^{-7}			
298.15	0.40314	7.7848×10^{-4}	-9.2506×10^{-5}				

where n_t is the absolute adsorption. There are only three parameters in Eq. (2): n_t^0, b and q. Coefficients c_i and c_j are not model parameters, but used to present "known values" for the convenience of computation. The point is how do we know the values of the absolute adsorption, n_t. The authors suggested an isotherm linearization strategy for studying supercritical adsorption (Zhou and Zhou, 1998) and a method to determine absolute adsorption from the experimental excess adsorption was developed afterwards (Zhou and Zhou, 2001e). Applying this method to Eq. (2), the authors successfully modeled the nitrogen isotherms on activated carbon (Zhou et al., 2001c).

The linear isotherms of nitrogen on silica gel are presented in Fig. 6. A reliable model can usually be formulated for linear plots, therefore, the absolute adsorption generated from the formulation is relatively dependable. Such a formulation for the linear isotherms was obtained and applied for the evaluation of the absolute adsorption n_t:

$$n_t = \frac{1}{100}\mathrm{Exp}\left[\mathrm{Exp}\left(\alpha + \frac{\beta}{\ln p}\right)\right] \tag{4}$$

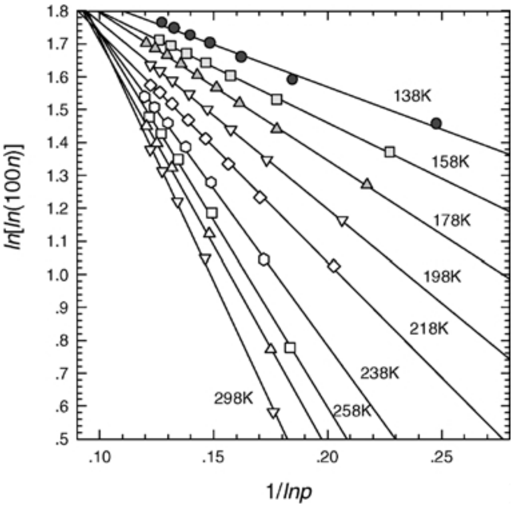

Figure 6. Linear isotherms in the supercritical region.

Parameters α and β are functions of temperature:

$$\alpha = 3.3433 - 2.2081 \times 10^{-2}\,T + 1.1302 \times 10^{-4}\,T^2 - 1.3649 \times 10^{-7}\,T^3\ (r^2 = 0.992) \tag{4.1}$$

$$\beta = -14.716 + 0.22843\,T - 1.2402 \times 10^{-3}\,T^2 + 1.5905 \times 10^{-6}\,T^3\ (r^2 = 0.996) \tag{4.2}$$

The adsorbed phase volume, V_a, is thus determined by substituting Eq. (4) into Eq. (3). The results were correlated with pressure by a polynomial function for each temperature just for the convenience of computation. The correlation coefficients are given in Table 4. There are eight (may be more or less) coefficients for evaluating n_t. These coefficients, as c_i and c_j mentioned above, could not be included into model parameters. They were used only for the determination of n_t, not for the excess adsorption n. The evaluated n_t can be applied elsewhere for other purpose, and the value of n_t can be determined from other way if there is any.

Fitting Eq. (2) to the experimental isotherms for 138.15–298.15 K, one obtains the value of the three model parameters by non-linear regression. The model-predicted isotherms are shown by continuous curves in Fig. 2. Apparently, it fits the experimental data quite well except the negative part of the isotherm at 138 K,

Table 4. Coefficients in the correlation of the adsorbed phase volume.

T (K)	c_j								
	c_0	c_1	c_2	c_3	c_4	c_5	c_6	c_7	c_8
138.15	1.2801	−4.4800	5.8730	−3.9017	1.4325	−0.30038	0.035785	-2.2535×10^{-3}	5.8246×10^{-5}
158.15	0.22395	−0.13117	0.027348	-1.3030×10^{-3}					
178.15	−0.059143	−0.014759	6.9399×10^{-3}	-3.2552×10^{-4}					
198.15	−0.077540	0.025156	-2.3898×10^{-4}						
218.15	−0.059799	0.022515	-3.7234×10^{-4}						
238.15	1.2919×10^{-3}	-5.1987×10^{-3}	4.1060×10^{-3}	-2.5347×10^{-4}					
258.15	−0.012785	-1.5330×10^{-3}	3.0920×10^{-3}	-1.8489×10^{-4}					
278.15	−0.060588	0.019855	-4.5480×10^{-4}						
298.15	−0.034528	0.017131	-3.4294×10^{-4}						

for which the dotted line seems more pertinent. However, the general disagreement of the model defined below is as less as ±3%, which is close to the experimental relative error of about ±2%.

$$d(\%) = \frac{1}{N_T} \sum_{j=1}^{N_T} \left(\frac{1}{N_m} \sum_{i=1}^{N_m} \frac{100 \times ABS(n_{\mathrm{cal}} - n_{\mathrm{exp}})}{n_{\mathrm{exp}}} \right) \tag{5}$$

where n_{cal} is the amount adsorbed calculated by the model; n_{exp} is the experimentally measured amount; N_m is the number of data at a given temperature; N_T is the number of isotherms. Besides, the satisfactory fit of Eq. (2) to the experimental isotherms confirmed the reliability of the method to determine the absolute adsorption.

The temperature dependent property of parameters is shown respectively in Figs. 7–9. Parameter n_t^0, the

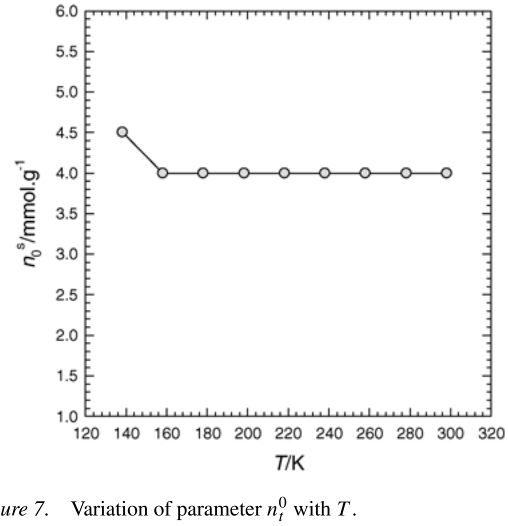

Figure 7. Variation of parameter n_t^0 with T.

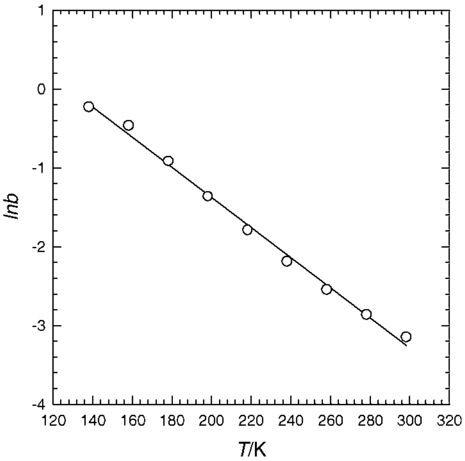

Figure 8. Variation of parameter b with T.

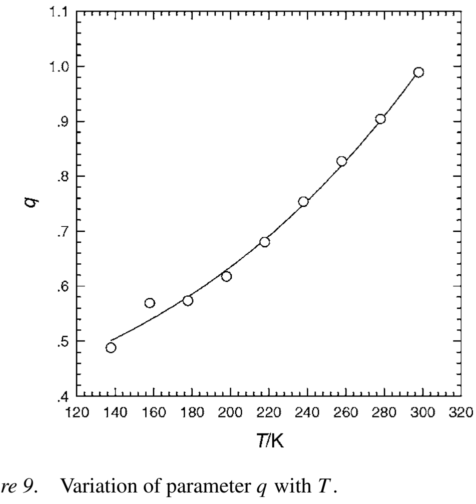

Figure 9. Variation of parameter q with T.

saturated absolute adsorption, is constant for most temperatures, but it increases to a higher value on approaching the critical temperature. The logarithm of parameter b decreases linearly with temperature, as observed at activated carbon (Zhou et al., 2001b). If, however, $\ln b$ varies linearly with the reciprocal temperature, i.e. $1/T$, the isosteric heat of adsorption would be evaluated. Therefore, how parameter b relates to the physical nature of the adsorption system is open for further study. Parameter q has similar meaning as the exponent parameter of other isotherm equations, but it takes value only in the range of 0 to 1 rendering it being a more appropriate index of the surface heterogeneity. Zero means the extreme heterogeneity, while unity means extreme uniformity. Parameter q increases with temperature because the heterogeneity of adsorbent *detected by the adsorbate molecules* must be less and less at ever increasing temperatures.

Additional information is obtained from the modeling. While the isotherms and the mechanisms implied by the isotherms are different for the adsorption of nitrogen on activated carbon (Zhou et al., 2001c) and on silica gel in the sub-critical region, the adsorption isotherms for the supercritical region can be well described by the same model, i.e., Eq. (2), in both cases. It leads logically to the conclusion: the adsorption mechanism for supercritical adsorption is identical no matter what kind of adsorbents was used and what type of isotherms may show for the sub-critical region.

4. Conclusions

1. The adsorption of nitrogen on silica gel is governed by different mechanisms in sub- and supercritical regions because a transformation of isotherms from type-II to type-I was observed.
2. The transition of adsorption mechanisms from the subcritical to the supercritical region is considerably different for the adsorption on activated carbon and on silica gel. All the isotherms in both regions belong to type-I on activated carbon, but type-II feature was shown for the isotherms on silica gel below the critical temperature. This difference is also shown on isotherm when expressed as n-ρ_g plot at a near critical temperature. The linear section coincided with the tangent of the isotherm arch for activated carbon, but the difference of isotherm types in two regions for silica gel results in a transition section ahead the linear section.
3. Although the isotherms in the subcritical region are of different type on silica gel and on activated carbon, the isotherms in the supercritical region can be satisfactorily modeled by the same model for both adsorbents. It proves a fact that the mechanism of the supercritical adsorption is identical no matter what kind of adsorbents is used.
4. The satisfactory fit of the proposed model achieved at different sets of experimental isotherms of supercritical adsorption confirmed the reliability of the method suggested for the evaluation of absolute adsorption. The new isotherm equation of the model contains three parameters, the meaning of which is physically reasonable.

Acknowledgment

This work is subsidized by the Special Funds of Major State Basic Research Projects (G2000026404) and supported by the National Natural Science Foundation of China (#29936100).

References

Agarwal, R.K. and J.A. Schwarz, “Analysis of High Pressure Adsorption of Gases on Activated Carbon by Potential Theory,” *Carbon*, **26**(6), 873–887 (1988).

Blümel, S., F. Köster, and G.H. Findenegg, “Physical Adsorption of Krypton on Graphite over a Wide Density Range,” *Chem. Soc., Faraday Trans.*, **2**(78), 1753–1764 (1982).

Cannon, J.S., “Hydrogen Vehicle Programs in the USA,” *Int. J. Hydrogen Energy*, **19**(11), 905–909 (1994).

Chen, X.S., B. McEnaney, T.J. Mays, J. Alcaniz-Monge, D. Cazorla-Amoros, and A. Linares-Solano, “Theoretical and Experimental Studies of Methane Adsorption on Microporous Carbons,” *Carbon*, **35**(9), 1251–1258 (1997).

Findenegg, G.H., “High Pressure Physical Adsorption of Gases,” *Fundamentals of Adsorption*, pp. 207–218 (1983).

Gregg, S.J. and K.S.W. Sing, *Adsorption, Surface Area and Porosity*, 2nd ed., Academic Press, London, 1982.

Humayun, R. and D.L. Tomasko, “High-Resolution Adsorption Isotherms of Supercritical Carbon Dioxide on Activated Carbon,” *AIChE Journal*, **46**(10), 2065–2075 (2000).

IUPAC, “Commission on Collid and Surface Chemistry Including Catalysis,” *Pure Appl. Chem.*, **57**, 603 (1985).

Jacobsen, R.T., R.B. Stewart, and M. Jahangiri, “Thermodynamic Properties of Nitrogen from the Freezing Line to 2000 K at Pressures to 1000 MPa,” *J. Phys. Chem. Ref. Data*, **15**(2), 735–909 (1986).

Jiang, S.Y., J.A. Zollweg, and K.E. Gubbins, “High-Pressure Adsorption of Methane and Ethane in Activated Carbon and Carbon Fibers,” *J. Phys. Chem.*, **98**, 5709–5713 (1994).

Keller, J.U., F. Dreisbach, H. Rave, R. Staudt, and M. Tomalla, “Measurement of Gas Mixture Adsorption Equilibria of Natural Gas

Compounds on Microporous Sorbents," *Adsorption*, **5**, 199–214 (1999).

Lösch, H.W., "Renaissance of Gravimetry in Metrology Under Controlled Environment—The Magnetic Suspension Balance," in *Business Briefing*, *Global Chemical Processing & Engineering Industry*, Feb. 1999, pp. 104–108.

Malbrunot, P., D. Vidal, J. Vermesse, R. Chahine, and T.K. Bose, "Adsorption Measurements of Argon, Neon, Krypton, Nitrogen, and Methane on Activated Carbon up to 650 MPa," *Langmuir*, **8**, 577–580 (1992).

Matranga, K.R., A.L. Myers, and E.D. Glandt, "Storage of Natural Gas by Adsorption on Activated Carbon," *Chem. Eng. Sci*., **47**(7), 1569–1579 (1992).

Menon, P.G., "Adsorption at High Pressure," *Chemical Reviews*, **68**, 277 (1968).

Noh, J.S., R.K. Agarwal, and J.A. Schwarz, "Hydrogen Storage Systems Using Activated Carbon," *Int. J. Hydrogen Energy*, **12**(10), 693–700 (1987).

Ozawa, S., S. Kusumi, and Y. Ogino, "Physical Adsorption of Gases at High Pressure, IV. An Improvement of the Dubinin-Astakhov Adsorption Equation," *Journal of Colloid and Interface Science*, **56**(1), 83–91 (1976).

Ruthven, D.M., F. Shamasuzaman, and K.S. Knaebel, *Pressure Swing Adsorption*, VCH Publishers, New York, 1994.

Specovius, J. and G.H. Findenegg, "Physical Adsorption of Gases at High Pressures: Argon and Methane onto Graphitized Carbon Black," *Ber. Bunsenges. Phys. Chem*., **82**, 174–180 (1978).

Tan, Z. and K.E. Gubbins, "Adsorption in Carbon Micropores at Supercritical Temperatures," *J. Phys. Chem*., **94**, 6061–6069 (1990).

Thommes, M., G.H. Findenegg, and M. Schoen, "Critical Depletion of a Pure Fluid in Controlled-Pore Glass. Experimental Results and Grand Canonical Ensemble Monte Carlo Simulation," *Langmuir*, **11**, 2137–2142 (1995).

Vermesse, J. and D. Levesque, "Monte Carlo Simulation of the Adsorption of Rare Gases at High Pressures," *J. Chem. Phys*., **101**(10), 9063–9071 (1994).

Vidal, D., P. Malbrunot, L. Guenggant, J. Vermesse, T.K. Bose, and R. Chahine, "Measurement of Physical Adsorption of Gases at High Pressure," *Rev. Sci. Instrum*., **61**(4), 1314–1318 (1990).

Wakasugi, Y., S. Ozawa, and Y. Ogino, "Physical Adsorption of Gases at High Pressure, V. An Extension of a Generalized Adsorption Equation to Systems with Polar Adsorbents," *Journal of Colloid and Interface Science*, **79**(2), 399–409 (1981).

Yang, R.T., *Gas Separation by Adsorption Processes*, Butterworths, London, 1987.

Zhou, L., J.-Sh. Zhang, and Y. Zhou, "A Simple Isotherm Equation for Modeling the Adsorption Equilibria on Porous Solids over Wide Range Temperatures," *Langmuir*, **17**(18), 5503–5507 (2001d).

Zhou, L. and Y. Zhou, "Linearization of Adsorption Isotherms for High Pressure Applications," *Chemical Engineering Science*, **53**(14), 2531–2536 (1998).

Zhou, L. and Y. Zhou, "A Mathematical Method for the Determination of Absolute Adsorption from Experimental Isotherms of Supercritical Gases," *Chinese J. of Chem. Eng*., **9**(1), 110–115 (2001e).

Zhou, L., Y. Zhou, Sh. Bai, Ch. Lü, and B. Yang, "Determination of the Adsorbed Phase Volume and its Application in Isotherm Modeling for the Adsorption of Supercritical Nitrogen on Activated Carbon," *J. Colloid & Interface Sci*., **239**, 33–38 (2001c).

Zhou, Y. and L. Zhou, "Experimental Study on High-Pressure Adsorption of Hydrogen on Activated Carbon," *Science in China (Series B)*, **39**(6), 598–607 (1996).

Zhou, Y., Sh. Bai, L. Zhou, and B. Yang, "Studies on the Physical Adsorption Equilibria of Gases on Porous Solids for a Wide Temperature Range Spanning the Critical Region—Adsorption on Microporous Activated Carbon," *Chinese Journal of Chemistry*, **19**(10), 943–948 (2001a).

Zhou, Y., Y. Sun, and L. Zhou, "An Experimental Study on the Adsorption Behavior of Gases on Crossing the Critical Temperature," *The 7th International Conference on Fundamentals of Adsorption*, Nagasaki, Japan, May 20–25, 2001b.